

New Approach to Obtain an Optimal Value for MQ-RBF Shape Parameter for the Nonlinear Analysis of Elastic Thin Plate



Mohammed Mohammed Hussein Al-Tholaia

University of Hafr AlBatin, Saudi Arabia

Submission: March 13, 2019; **Published:** March 28, 2019

***Corresponding author:** Mohammed Mohammed Hussein Al-Tholaia, University of Hafr AlBatin, Saudi Arabia

Abstract

A new approach in using a multi-quadric radial basis function (MQ-RBF) in the analysis of nonlinear behaviour of elastic thin plate is provided. The approach provides a new method to obtain an optimal value of the shape parameter, c , involved in the (MQ-RBF). The shape parameter c plays a very important role in the accuracy and stability of the solution. The approach uses approximate exact linear solutions of linear analysis of the thin plates as standpoint toward the calculation of the optimal c value. Then, the optimal c values were implemented in the analysis of nonlinear thin plate behaviour. Combinations of different boundary conditions (simply, and clamped), for a square thin plate under uniform distribution loads were analysed. The accuracy of the adopted approach has been validated by comparing the results with FEM solutions. The comparison shows that the approach can be used effectively in obtaining the optimal value of c .

Keywords: Thin plate; MQRBF; Nonlinear analysis; Shape parameter; Finite element method; Boundary element method

Introduction

The analysis of the elastic thin plate under different loads with various boundary conditions is provided by two main theories (small and large deflection) [1,2]. In the small deflection theory, linear analysis is adopted. For such cases, approximate exact solutions for different boundary conditions, loads and shapes are available like the ones in Timoshenko book [1]. However, the nonlinear behaviour analysis is adopted by the large deflection theory [1]. The nonlinearity comes from the coupling of the three governing partial differential equations as described in [1,2] for the transverse and lateral deformations. Some attempts to find approximate exact analytical and semi-analytical solutions for some cases of the large deflection analysis are provided [3-5]. However, several assumptions and restrictions were employed in order to have such solutions which make those attempts very limited and not valid to cover wide range of variation of real problems. On the other hand, and to handle numerous real problems, numerical solutions were adopted. Numerous numerical methods are available such as finite element method (FEM), boundary element method (BEM), finite difference method (FDM), etc [6-12]. The most common numerical method is the FEM which has been approved as a very good method in terms of the accuracy and flexibility. However, and despite of the intensive

research in FEM, there are still some problems raised such as the ones because of the distortion from the large deflection which needs re-meshing during the analysis.

To overcome the re-meshing generation problems, different researchers have adopted meshless or mesh-free numerical methods in the last decades [13-29]. Several types of such methods are adopted to solve different problems. According to the literature, the MQ-RBF based meshless method is the best method that can handle the solution of the partial differential equation applications. However, the shape parameter, c , involved in the MQ-RBF plays a very important role in the accuracy and stability of the solution. The main concern is the determination an optimal value of c [13-15]. From the literature, several approaches and attempts to get optimal values of c are provided [13,28-34]. Those approaches depend mainly on the available data for which MQ-RBF is used as an interpolant. In this paper, a different approach is adopted to get the optimal value of c using the linear exact solution of the thin plates. The description of the method is provided in section 2. The method has been tested using several examples such as simply, clamped, and simply clamped square plate under uniform distribution loads. The results show that the adopted method is an effective tool to get the optimal value of c .

Method Description

The method of finding an optimal c value using exact linear solution for elastic thin plate is summarized as follows:

- 1) Implement the exact solution and get the deflection function, w.
- 2) Divide the plate to specific number of nodes (in the domain and in the boundary).
- 3) Find the deflections for the whole nodes from the exact solution obtained from Step (1).
- 4) Represent w by MQ-RBF as it is shown in Section 3.
- 5) Assume initial value for c, let it equal to the minimum distance between the nodes.
- 6) Apply the governing partial differential equation for the transverse deflection, w which is $\nabla^4 w = \frac{q}{D}$.
- 7) Apply the boundary conditions according to the specified problem
- 8) Solve the developed equations in the steps (6) and (7) to get the required coefficients in step (4)
- 9) Calculate the difference between the obtained deflections in step (4) and step (3).
- 10) Change the value of c with a specific scheme and repeat steps from 6 to 9
- 11) Repeat step 10 for several values of c and then take the optimal c values which make the calculated difference in step 9 within 5%.

Formulation of the Problem

Governing Equations and Boundary Conditions

For an elastic thin plate undergoing large deformation, the governing equilibrium equations are expressed in terms of the out of plane deformation, w and the in-plane deformation u and v. Here is the summary of the formulations and their boundary conditions as follows [28, 29];

$$L_{11}(u) + L_{12}(v) = NL_1(w) \quad (1)$$

$$L_{21}(u) + L_{22}(v) = NL_2(w) \quad (2)$$

$$\nabla^4 w = \frac{q}{D} + NL_3(u, v, w) \quad (3)$$

Where,

$$L_{11} = \frac{2\partial_{xx} + (1-\nu)\partial_{yy}}{2(1-\nu^2)}$$

$$L_{12} = \frac{2\partial_{xy}}{2(1-\nu)}$$

$$L_{22} = \frac{2\partial_{yy} + (1-\nu)\partial_{xx}}{2(1-\nu^2)}$$

$$NL_1(w) = -\frac{(1+\nu)w_{xy}w_y + w_x(2w_{xx} + (1-\nu)w_{yy})}{2(1-\nu^2)}$$

$$NL_2(w) = -\frac{(1+\nu)w_{xy}w_x + w_y(2w_{yy} + (1-\nu)w_{xx})}{2(1-\nu^2)}$$

$$NL_3(u, v, w) = \frac{Etw_{xy}}{D(1+\nu)}(u_y + v_x + w_x w_y) + \frac{Etw_{xx}}{2D(1+\nu^2)}(2u_x + w_x^2 + \nu(2v_y + w_y^2)) + \frac{Etw_{yy}}{2D(1+\nu^2)}(2v_y + w_y^2 + \nu(2u_x + w_x^2))$$

Subscript variables in the previous equations represent partial differentiation with respect to the variables.

$$D = \frac{Et^3}{12(1-\nu^2)} ; t \text{ is plate thickness, } \nu \text{ is poisson's ratio, } E \text{ is}$$

Young's Modulus and q is uniform load

A. Boundary Conditions

Two main types of boundary conditions can be categorized for large deformation of thin plates. The out-of-plane boundary conditions are found in both small and large deflection theories whereas the in-plane boundary conditions are found only in the large deformation theory.

- a. For the in-plane boundary conditions, $u = v = 0$.
- b. For the out-of-plane boundary conditions, there are two primary boundary conditions at each point in the boundary as follows:

$$BC_{w1}(w) = 0$$

$$\text{where } BC_{w1}(w) = \begin{cases} w, & \text{for clamped and simple edge} \\ v_n, & \text{for free edge} \end{cases}$$

$$BC_{w2}(w) = 0,$$

$$\text{Where; } BC_{w2}(w) = \begin{cases} \frac{\partial w}{\partial n}, & \text{for clamped edge} \\ M_n, & \text{for simple and free edge} \end{cases}$$

$$M_n = -D \left\{ \nu \nabla^2 w + (1-\nu)(n_x^2 \frac{\partial^2 w}{\partial x^2} + n_y^2 \frac{\partial^2 w}{\partial y^2} + 2n_x n_y \frac{\partial^2 w}{\partial x \partial y}) \right\}$$

Regarding the shear, V_n , it was divided into two components

(Linear part V_n^L , and Nonlinear part V_n^{NL}) as follows;

$$V_n^L = -D \left\{ (n_y(1-n_x^2(v-1))) \frac{\partial^3 w}{\partial y^3} + (n_x(1-n_y^2(v-1))) \frac{\partial^3 w}{\partial x^3} + n_x(-2n_x^2(v-1) + 2n_y^2(v-1) + \nu) \frac{\partial^3 w}{\partial y \partial x} + n_y(n_x^2(v-1) - 2n_y^2(v-1) + \nu) \frac{\partial^3 w}{\partial x \partial y} \right\}$$

$$V_n^{NL} = \frac{Et}{12(-1+\nu)} \left[\begin{aligned} & -12n_y \frac{\partial v}{\partial y} \frac{\partial w}{\partial y} - 6n_y \left(\frac{\partial w}{\partial x} \right)^2 \frac{\partial w}{\partial y} - 6n_y \left(\frac{\partial w}{\partial y} \right)^3 + 6n_y(-1+\nu) \frac{\partial u}{\partial y} \frac{\partial w}{\partial x} \\ & + 6n_y(-1+\nu) \frac{\partial v}{\partial x} \frac{\partial w}{\partial x} - 12n_x \nu \frac{\partial u}{\partial x} \frac{\partial w}{\partial y} - 12n_x \frac{\partial u}{\partial x} \frac{\partial w}{\partial x} - 6n_x \left(\frac{\partial w}{\partial x} \right)^3 \\ & + 6n_x(-1+\nu) \frac{\partial u}{\partial y} \frac{\partial w}{\partial y} + 6n_x(-1+\nu) \frac{\partial v}{\partial x} \frac{\partial w}{\partial y} - 6n_x \left(\frac{\partial w}{\partial y} \right)^2 \frac{\partial w}{\partial x} - 12n_x \nu \frac{\partial v}{\partial y} \frac{\partial w}{\partial x} \end{aligned} \right]$$

where n_x and n_y represent the unit vector components normal to the boundary, x and y respectively.

RBF Formulations

The nature and definition of RBF depends on the radial distances between the points. For 2-Dimensional problem like the one in this study, x and y axes are considered. For general body shape, it is divided into two main parts, the domain (Ω) and the boundary (Γ). Both the domain and the boundary are divided into several points (x_D, y_D) and (x_B, y_B) respectively as shown in Figure 1.

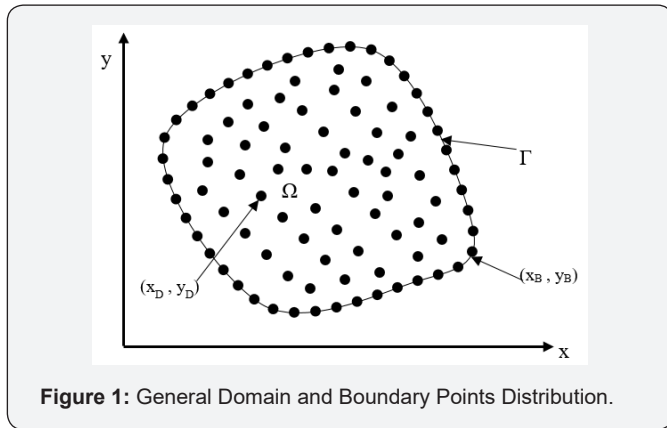


Figure 1: General Domain and Boundary Points Distribution.

The number of points in the domain and boundary denoted by N_D and N_B respectively. The total points $N_p = N_D + N_B$. MQ-RBF is defined as: $\phi(\|\underline{x} - \underline{x}^j\|) = \sqrt{(\underline{x} - \underline{x}^j)^2 + c^2}$, where c is the shape variable or parameter.

To solve the thin plate problem using MQ-RBF, the out of plane deformation, w , and the in-plane deformations, u and v , are represented by a combination of MQ-RBF with constants as described below.

$$w(\underline{x}) = \sum_{j=1}^{N_D} a_w^j BC_{w1}(\phi(\|\underline{x} - \underline{x}_D^j\|)) + \sum_{j=1}^{N_B} a_w^{j+N_D} BC_{w2}(\phi(\|\underline{x} - \underline{x}_B^j\|)) + \sum_{j=1}^{N_D} a_w^{j+2N_B} \phi(\|\underline{x} - \underline{x}_D^j\|)$$

$$u(\underline{x}) = \sum_{j=1}^{N_p} a_u^j \phi(\|\underline{x} - \underline{x}_p^j\|)$$

$$v(\underline{x}) = \sum_{j=1}^{N_p} a_v^j \phi(\|\underline{x} - \underline{x}_p^j\|)$$

Where, a_w^j, a_u^j, a_v^j are constants and can be determined by applying the governing equations and boundary conditions. For the purpose of programming the solution, the governing equations as well as the boundary conditions for both out and in-plane deformations are summarized and organized in matrices forms as follows:

The out of plane matrices;

$$\begin{bmatrix} BC_{w1}(BC_{w1}(\phi)) & BC_{w1}(BC_{w2}(\phi)) & BC_{w1}(\phi) \\ BC_{w2}(BC_{w1}(\phi)) & BC_{w2}(BC_{w2}(\phi)) & BC_{w2}(\phi) \\ (\nabla^4)(BC_{w1}(\phi)) & (\nabla^4)(BC_{w2}(\phi)) & (\nabla^4)(\phi) \end{bmatrix} * \begin{bmatrix} a_w^j, j=1, N_D \\ a_w^{j+N_D}, j=1, N_B \\ a_w^{j+2N_B}, j=1, N_D \end{bmatrix} = \begin{bmatrix} BC_{w1}(w) \\ BC_{w2}(w) \\ \frac{q}{D} + NL_3(u, v, w) \end{bmatrix} \quad (4)$$

They are denoted by: $[A_w] \{a_w\} = \{R_w\}$

$$\begin{bmatrix} \phi & \phi & 0 & 0 \\ L_{11}(\phi) & L_{11}(\phi) & L_{12}(\phi) & L_{12}(\phi) \\ 0 & 0 & \phi & \phi \\ L_{21}(\phi) & L_{21}(\phi) & L_{22}(\phi) & L_{22}(\phi) \end{bmatrix} * \begin{bmatrix} a_u^j, j=1, N_B \\ a_u^{j+N_B}, j=1, N_D \\ a_v^j, j=1, N_B \\ a_v^{j+N_B}, j=1, N_D \end{bmatrix} = \begin{bmatrix} 0 \\ NL_1(w) \\ 0 \\ NL_2(w) \end{bmatrix} \quad (5)$$

They are denoted by: $[A_{uv}] \{a_{uv}\} = \{R_{uv}\}$

The procedure of the solution of equations (4) and (5) is as follows:

1. Input data such as geometry, boundary conditions, materials, loads, the optimal c value calculated in section 2 above.
2. Calculate A_w and A_{uv}
3. Calculate the inverses of A_w and A_{uv}
4. Apply load increment
5. Initialize the nonlinear terms ($NL_1(w)$, $NL_2(w)$, VNL , and $NL_3(w, u, v)$)
6. Calculate w and a_{uv}
7. Get w, u , and v
8. Calculate w at the centroid of the plate
9. Evaluate the nonlinear terms, mentioned in Step 4
10. Repeat steps 6 to 8
11. Calculating the error which is $= \left| \frac{w_8 - w_{10}}{w_8} \right| * 100$
12. If the error is $< 0.05\%$, go to Step 4 to apply the new increment and repeat the steps from 5 to 12 until the whole load is applied.
13. If the error is not less than 0.05% , repeat steps from 9 to 12.
14. Print the results and stop the program.

Numerical Examples

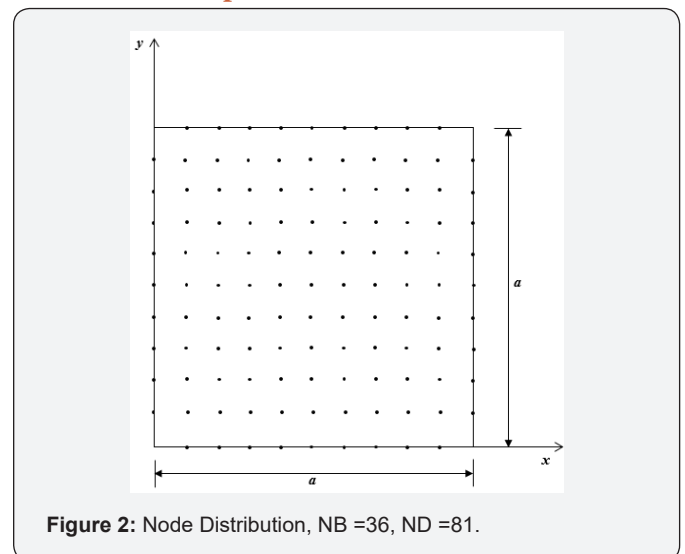


Figure 2: Node Distribution, NB =36, ND =81.

General information has been used for all examples. The material dimensionless properties are the same, which are as follows: Young's modulus $E=10000$, Poisson's Ratio $\nu=0.3$. The plate thickness is $t=0.1$. Uniform node distribution has been adopted for all as it is shown in the Figure 2 below.

In addition, the results of the solutions (exact, MQ-RBF for linear analysis, MQ-RBF for Nonlinear analysis, and Finite Element Analysis for nonlinear analysis), are shown in tables and charts. For the linear analyses, the results include optimal c values, deflections, w , from exact and MQRBF solutions at the centroid of the plates. Comparisons between the corresponding solution results are shown as well by calculating the differences. However, for the nonlinear analyses, the deflection, the bending and membrane stresses results for both the MQRBF and FEM solutions in tables and charts. In addition, the differences between the MQ-RBF and FEM solutions are provided for validation.

Clamped-Clamped Supported Square Plate (CCS)

A square plate with dimensions $a=b$ and clamped supports on all sides, is analysed under dimensionless uniform load, $q=160$. The exact solution for the nonlinear analysis is given by Timoshenko & Woinowsky-Kreiger [1]. (Figure 3)

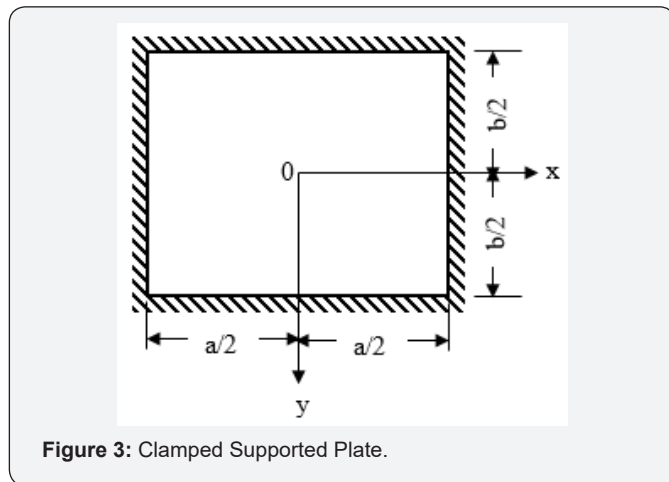


Figure 3: Clamped Supported Plate.

$$w = -\frac{a^2}{2\pi^2 D} \sum_{m=1,3,5,\dots}^{\infty} E_m \frac{-1^{-m}}{m^2 \cosh \alpha_m} \cos \frac{m\pi x}{a} \left(\frac{m\pi y}{a} \sinh \frac{m\pi y}{a} - \alpha_m \tanh \alpha_m \cosh \frac{m\pi y}{a} \right);$$

$$\alpha_m = \frac{m\pi b}{2a}; E_1 = 0.3722K; E_3 = -0.0380K; E_5 = -0.0178K; E_7 = -0.0085K; K = \frac{-4qa^2}{\pi^2}$$

The boundary conditions are; $w = \frac{\partial w}{\partial n} = u = v = 0$, on all boundaries.

Table 2: Deflection, Bending and Membrane Stresses Differences of MQRBF and FEM, CCS.

Clamped -Clamped Supported, $c = 0.3$ at the Center of the Plate									
q	w/t			σ_b			σ_m		
	FEM	RBF	Diff%.	FEM	RBF	Diff%.	FEM	RBF	Diff%.
20	0.263214	0.26686	1.38521	2.62172	2.53949	3.136622	0.236111	0.224104	5.085426
40	0.493113	0.490979	0.432794	4.69495	4.59033	2.228371	0.795137	0.75909	4.533426
60	0.675533	0.670057	0.810678	6.21087	6.12052	1.454752	1.473083	1.42945	2.962024

The results of the analysis using the exact solution and the MQ-RBF for the deflections at the centre of the plate for $q=60$ are given in Table 1. The results contain the exact, MQ-RBF, differences as percent and the corresponding c values. From the results shown in Table 1, the optimal c values are 0.2 and 0.8.

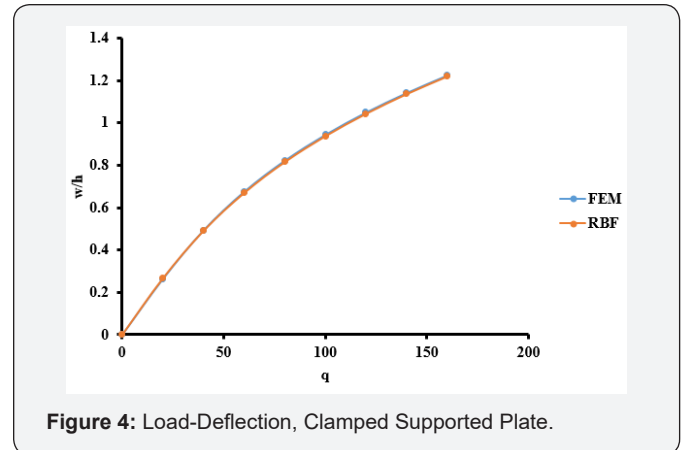


Figure 4: Load-Deflection, Clamped Supported Plate.

The optimal c values obtained from Table 1 are used in the large deflection analysis for the plate. The total load, $q = 160$, has been applied incrementally with load increment of 20. The dimensionless results of deflection, bending stresses, and membrane stresses are shown in Table 2 and Figures 4-6. Comparison between the MQ-RBF and FEM is included in Table 2 as differences in percent.

Table 1: MQRBF-Exact differences and c values, CCS.

c	w/t		
	Exact	RBF	Diff. %
0.1	0.8315	0.48949	41.1317
0.2	0.8315	0.82254	1.07712
0.3	0.8315	0.8249	0.79365
0.4	0.8315	0.82431	0.86425
0.5	0.8315	0.82465	0.82288
0.6	0.8315	0.82538	0.73544
0.7	0.8315	0.82628	0.6272
0.8	0.8315	0.81857	1.55433
0.9	0.8315	0.87272	4.95755
1	0.8315	-44.177	5412.95

80	0.822271	0.815894	0.775489	7.33652	7.22966	1.456537	2.173673	2.12878	2.065294
100	0.944636	0.938339	0.666555	8.20351	8.13548	0.829224	2.863406	2.81739	1.607039
120	1.0498	1.04392	0.560082	8.89526	8.78118	1.282491	3.532043	3.49108	1.159742
140	1.14228	1.136906	0.47045	9.46399	9.57122	1.132979	4.177477	4.06041	2.802339
160	1.22503	1.220171	0.396674	9.94333	9.86825	0.7551	4.800432	4.78148	0.394801

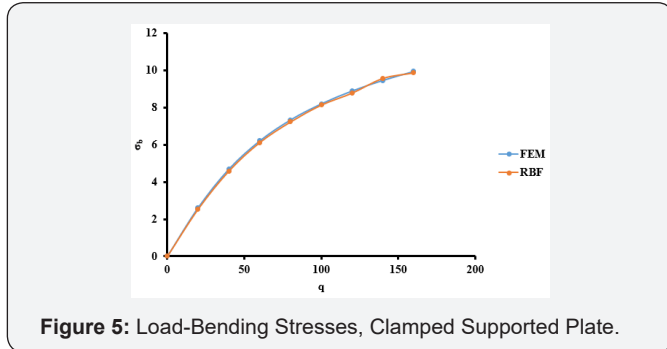


Figure 5: Load-Bending Stresses, Clamped Supported Plate.

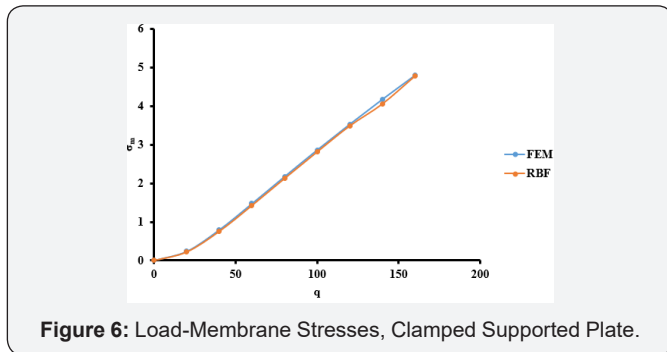


Figure 6: Load-Membrane Stresses, Clamped Supported Plate.

Simply – Simply Supported Square Plate (SSS)

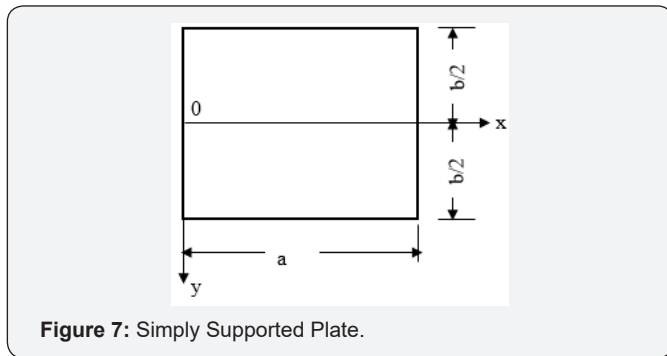


Figure 7: Simply Supported Plate.

A square plate with dimensions $a = b$ and simple supports on all sides, is analysed under dimensionless uniform load, $q = 48$.

Table 4: Deflection, Bending and Membrane Stresses Differences of MQRBF and FEM, SSS.

Simply -Simply Supported, $c = 0.60$ at the Centre of the Plate									
q	w/t/center			σ_b			σ_m		
	FEM	RBF	Diff%.	FEM	RBF	Diff%.	FEM	RBF	Diff%.
6	0.245736	0.242958	1.130428	1.58066	1.56605	0.924025	0.182955	0.1794	1.942876
12	0.423934	0.422335	0.377177	2.67895	2.67998	0.038188	0.545533	0.543803	0.317141
18	0.553529	0.559277	1.038464	3.43679	3.49007	1.550148	0.931861	0.933398	0.165038
24	0.654631	0.652656	0.301672	4.00045	4.01187	0.285448	1.305935	1.328285	1.711414

The exact solution for the nonlinear analysis is given by Timoshenko & Woinowsky-Kreiger [1]: (Figure 7)

$$w = \frac{4qa^2}{\pi^5 D} \sum_{m=1,3,5,\dots}^{\infty} \frac{1}{m^5} \left(1 - \frac{\alpha_m \tanh \alpha_m + 2}{2 \cosh \alpha_m} \cosh \frac{2\alpha_m y}{b} + \frac{a_m}{2 \cosh \alpha_m} \frac{2y}{b} \sinh \frac{2\alpha_m y}{b} \right) \sin \frac{m\pi x}{a}$$

The boundary conditions are; $w = M_n = u = v = 0$, on all boundaries.

Table 3: MQRBF-Exact differences and c values, SSS.

c	w/t		
	Exact	RBF	Diff.
0.1	0.80773	0.4494	44.3624
0.2	0.80773	0.83953	3.93595
0.3	0.80773	0.8091	0.16862
0.4	0.80773	0.79716	1.30872
0.5	0.80773	0.79296	1.82919
0.6	0.80773	0.7921	1.93566
0.7	0.80773	0.79264	1.86819
0.8	0.80773	0.79365	1.74365
0.9	0.80773	0.79942	1.02893
1	0.80773	0.93549	15.8162

The results of the analysis using the exact solution and the MQ-RBF for the deflections at the center of the plate for $q=18$ are given in Table 3. The results contain the exact, MQ-RBF, differences as percent and the corresponding c values. From the results shown in Table 1, the optimal c values are 0.3 to 0.9.

The optimal c values obtained from Table 1 are used in the large deflection analysis for the plate. The total load, $q=48$, has been applied incrementally with load increment of 6. The dimensionless results of deflection, bending stresses, and membrane stresses are shown in Table 4 and Figures 8-10. Comparison between the MQ-RBF and FEM is included in Table 4 as differences in percent.

30	0.737872	0.733497	0.592975	4.44582	4.44909	0.073504	1.662181	1.693724	1.897673
36	0.808957	0.797764	1.383582	4.81298	4.78192	0.64526	2.001238	2.052363	2.55463
42	0.871247	0.86548	0.661877	5.12513	5.13308	0.155222	2.324955	2.363551	1.660072
48	0.926875	0.92195	0.531409	5.39672	5.41589	0.355194	2.635213	2.672072	1.398707

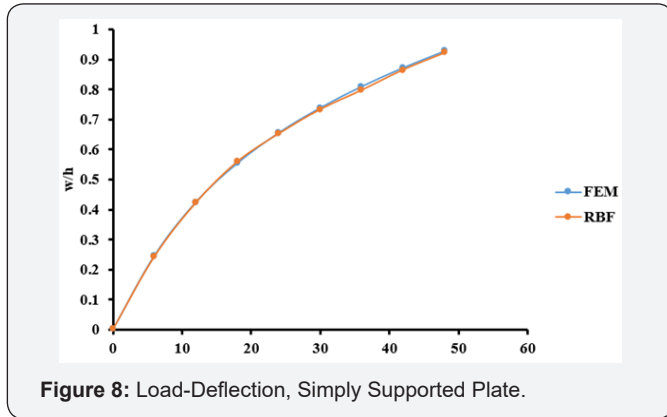


Figure 8: Load-Deflection, Simply Supported Plate.

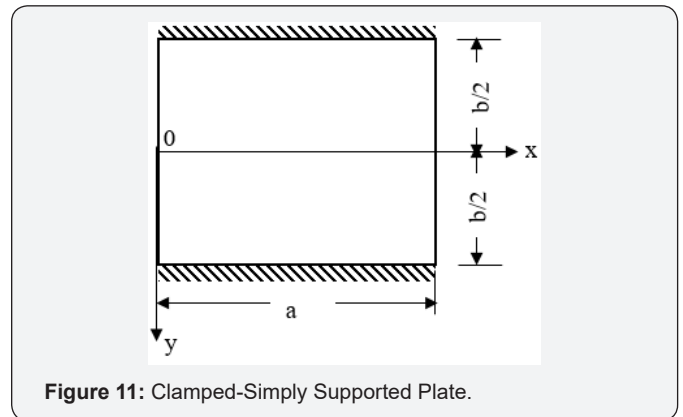


Figure 11: Clamped-Simply Supported Plate.

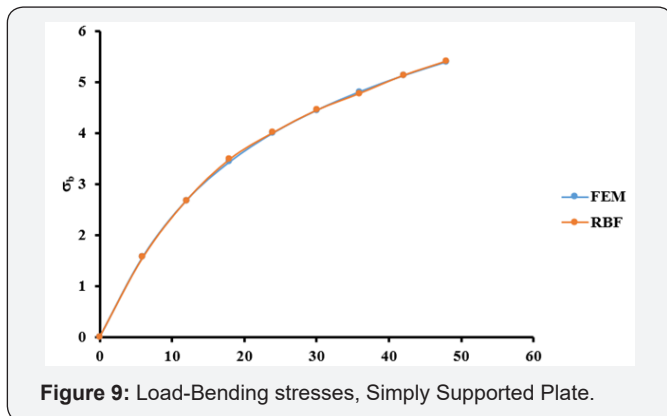


Figure 9: Load-Bending stresses, Simply Supported Plate.

The boundary conditions are;

On simple support sides $w = M_n = u = v = 0$ and

On clamped supports sides $w = \frac{\partial w}{\partial n} = u = v = 0$.

The results of the analysis using the exact solution and the MQ-RBF for the deflections at the center of the plate for $q=36$ are given in Table 5. The results contain the exact, MQ-RBF, differences as percent and the corresponding c values. From the results shown in Table 1, the optimal c values are 0.2 to 0.9.

Table 5: MQRBF-Exact differences and c values, CSS.

c	w/t		
	Exact	RBF	Diff.
0.1	0.77125	0.43916	43.0587
0.2	0.77125	0.75693	1.85711
0.3	0.77125	0.75127	2.5915
0.4	0.77125	0.74822	2.98631
0.5	0.77125	0.74779	3.04233
0.6	0.77125	0.74846	2.95532
0.7	0.77125	0.74945	2.82683
0.8	0.77125	0.75405	2.23079
0.9	0.77125	0.78143	1.31928
1	0.77125	0.66773	13.4227

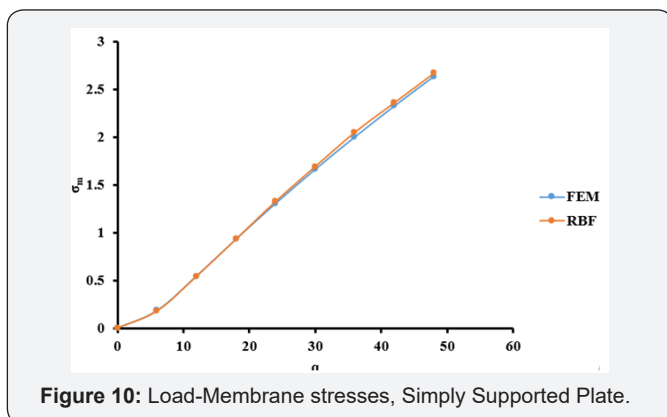


Figure 10: Load-Membrane stresses, Simply Supported Plate.

Clamped-Simply Supported Square Plate (CSS)

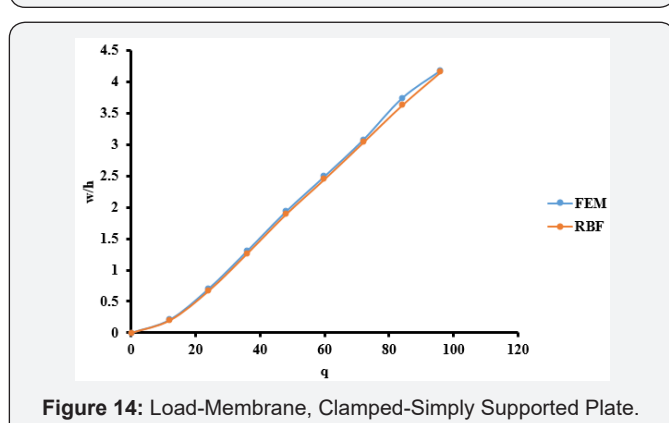
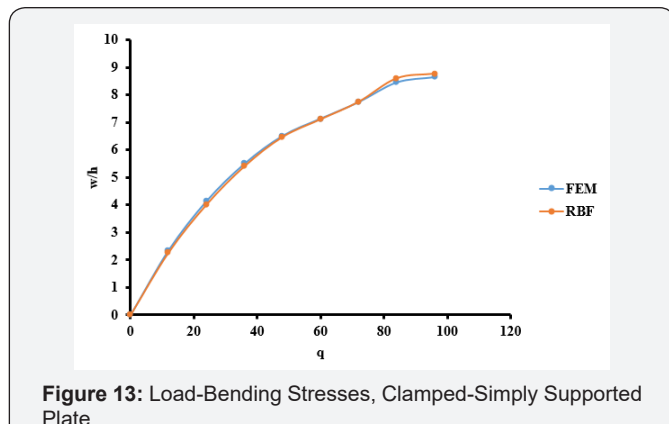
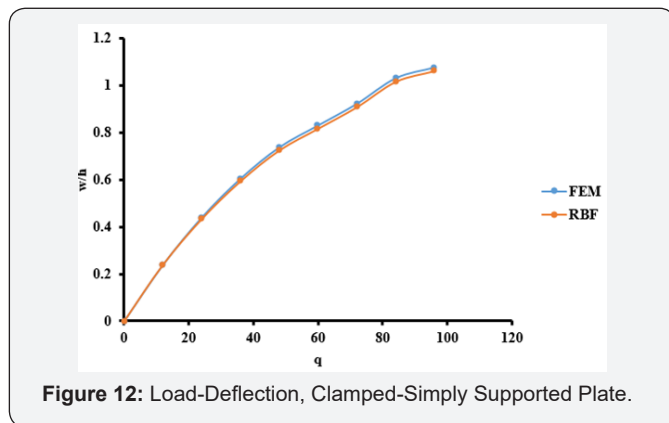
A square plate with dimensions $a=b$ and clamped supports on two sides and simply supports on the other two sides, is analysed under dimensionless uniform load, $q=96$. The exact solution for the nonlinear analysis is given by Timoshenko & Woinowsky-Krieger [1] (Figure11)

$$w = \frac{2qa^2}{\pi^2 D} \sum_{m=1,3,5,\dots}^{\infty} \frac{\sin \frac{m\pi x}{a}}{m^5 \cosh \alpha_m} \frac{\alpha_m - \tanh \alpha_m (1 + \alpha_m \tanh \alpha_m)}{\alpha_m - \tanh \alpha_m (\alpha_m \tanh \alpha_m - 1)} \left(\frac{m\pi y}{a} \sinh \frac{m\pi y}{a} - \alpha_m \tanh \alpha_m \cosh \frac{m\pi y}{a} \right)$$

The optimal c values obtained from Table 1 are used in the large deflection analysis for the plate. The total load, $q = 96$, has been applied incrementally with load increment of 12. The dimensionless results of deflection, bending stresses, and membrane stresses are shown in Table 6 and Figures 12-14. Comparison between the MQ-RBF and FEM is included in Table 6 as differences in percent.

Table 6: Deflection, Bending and Membrane Stresses Differences of MQRBF and FEM, CSS.

Clamped -Simply Supported, $c = 0.2$ at the Centre of the Plate									
q	w/t/Centre			σ_b			σ_m		
	FEM	RBF	Diff%.	FEM	RBF	Diff%.	FEM	RBF	Diff%.
12	0.238768	0.239679	0.381396	2.35469	2.26888	3.644117	0.212062	0.201278	5.085426
24	0.439878	0.433638	1.418608	4.14663	4.00967	3.302997	0.702274	0.670437	4.533426
36	0.604916	0.594071	1.792751	5.50655	5.40049	1.926049	1.306033	1.267348	2.962024
48	0.737685	0.724717	1.75791	6.51665	6.45993	0.870423	1.930762	1.890886	2.065294
60	0.830761	0.817053	1.650054	7.14315	7.10016	0.601822	2.493292	2.453224	1.607039
72	0.922713	0.90846	1.544635	7.741	7.73527	0.074046	3.073721	3.038074	1.159742
84	1.031081	1.01607	1.455891	8.45811	8.58722	1.52642	3.733474	3.628849	2.802339
96	1.076425	1.06154	1.382846	8.65063	8.75654	1.224302	4.176343	4.159855	0.394801



Results Discussion

As shown in the results in Section 4, one can get several interesting observations. For the clamped supported plate (CCS), from Table1, the minimum difference between the exact solution and the MQ-RBF solution for the deflection at the centre of the plate is 0.627 % at value of $c = 0.7$. The differences are less than 5 % for the values of c ranging from 0.2 to 0.8. As a result, the large deflection analysis has been done for the plate using several values of c for the mentioned range. In Table 2, the results of the deflection, bending and membrane stresses at the centre of the plate from both FEM and MQ-RBF at $c=0.3$ and their differences are provided. It has been noticed that, the maximum difference of the deflections is 1.4% and the bending stresses is 3%. However, the maximum difference of the membrane stresses is 5%. In general, the differences are within 5%. From Figures 4-6, it is clear that the results from the MQRBF and FEM are almost the same which means that the differences are so small.

Likewise, the simply supported plate has the same trend. From Table 3, the minimum difference is 0.1686% at $c=0.3$. Also, the differences are still less than 5% for the c values ranging from 0.2 to 0.9. Using the optimal values of c , the nonlinear analysis for the simply supported plate has been carried out and the results of the deflection, bending and membrane stresses at the centre of the plate from both FEM and MQ-RBF at $c=0.6$ and their differences are provided in Table 4. It was noticed that, all the differences are within 5%. In addition, the graphs shown in Figures 8-10 show excellent agreement between the FEM and MQRBF solutions. The same observations were noticed from the third example which is the Clamped-Simply supported plate (CSS). All the differences are within 5% for the values of c ranging from 0.2 to 0.9 as shown in Table 5 and shown in Table 6 for the nonlinear analysis at $c=0.2$. A very good agreement between the MQRBF and FEM solution is satisfied as shown in Figures 12-14.

Conclusion

From this study, it can be concluded that the adopted approach of finding optimal c values from the comparison of the available approximate exact solutions and MQRBF solution for the linear analysis of thin plate has been demonstrated to be an

effective tool. The range of the optimal c values are between 0.2 to 0.8, for the three different boundary conditions (clamped (CCS), simply (SSS), and clamped-simply (CSS)), used in the study. The optimal c values were used in the nonlinear analysis of the three examples and then validated by the FEM solutions. A very good agreement between the MQRBF and FEM solutions is observed for the three different examples. Because of the availability of approximate linear exact solutions for most of the engineering problems, the adopted approach can be utilized for other cases easily to obtain optimal c values, which can be used in the analysis of the nonlinear problems with good accuracy.

References

1. Timoshenko PS, Woinowsky-Kreiger S (1959) Theory of Plates and Shells. McGraw-Hill, New York, NY, USA.
2. Augural C (1999) Stresses in Plates and Shells. McGraw-Hill, New York, NY, USA.
3. Little GH (1999) Efficient large deflection analysis of rectangular plates with general transverse form of displacement. *Computers and Structures*71(3): 333-352.
4. Little GH (1999) Large deflections of rectangular plates with transverse edges remaining straight. *Computers and Structures* 71(3): 353-357.
5. Ramachandra LS, Roy D (2001) A novel technique in the solution of axisymmetric large deflection analysis of a circular plate. *Journal of Applied Mechanics* 68(5): 814-816.
6. Papakaliatakis G, Simos TE (1997) A finite difference method for the numerical solution of fourth-order differential equations with engineering applications. *Computers & Structures*65(4): 491-495.
7. Duan M, Mahendran M (2003) Large deflection analyses of skew plates using hybrid/mixed finite element method. *Computers and Structures*81(13): 1415-1424.
8. Szilard R (2004) Theories and Applications of Plate Analysis. John Wiley & Sons, New Jersey, NJ, USA.
9. Katsikadelis JT, Nerantzaki MS (1994) Non-linear analysis of plates by the analog equation method. *Computational Mechanics*14(2): 154-164.
10. El-Zafrany A, Fadhil S, Debbih M (1995) An efficient approach for boundary element bending analysis of thin and thick plates. *Computers & Structures*56(4): 565-576.
11. Luo ACJ, Mote J (2003) Asymmetric responses of rotating, thin disks experiencing large deflections. *Computers & Mathematics with Applications* 45(1-3): 217-228.
12. Byklum E, Amdahl J (2002) A simplified method for elastic large deflection analysis of plates and stiffened panels due to local buckling. *Thin-Walled Structures*40(11): 925-953.
13. Hardy RL (1971) Multiquadric equations of topography and other irregular surfaces. *Journal of Geophysical Research* 76(8): 1905-1915.
14. Kansa EJ (1990) Multiquadrics-a scattered data approximation scheme with applications to computational fluid-dynamics. I. Surface approximations and partial derivative estimates. *Computers & Mathematics with Applications* (8-9): 127-145.
15. Kansa EJ (1990) Multiquadrics-a scattered data approximation scheme with applications to computational fluid-dynamics—II solutions to parabolic, hyperbolic and elliptic partial differential equations. *Computers & Mathematics with Applications*19(8-9): 147-161.
16. Nayroles B, Touzot G, Villon P (1992) Generalizing the finite element method: diffuse approximation and diffuse elements. *Computational Mechanics* 10(5): 307-318.
17. Belytschko T, Lu YY, Gu L (1994) Element-free Galerkin methods. *International Journal for Numerical Methods in Engineering* 37(2): 229-256.
18. Liu WK, Jun S, Zhang YF (1995) Reproducing kernel particle methods. *International Journal for Numerical Methods in Fluids*20(8-9): 1081-1106.
19. Onate E, Idelsohn S, Zienkiewicz OC, Taylor RL (1996) A finite point method in computational mechanics. Applications to convective transport and fluid flow. *International Journal for Numerical Methods in Engineering* 39(22): 3839-3866.
20. Atluri SN, Zhu T (1998) A new Meshless Local Petrov-Galerkin (MLPG) approach in computational mechanics. *Computational Mechanics* 22(2): 117-127.
21. Liu GR, Gu YT (2003) A meshfree method: meshfree weak strong (MWS) form method, for 2-D solids. *Computational Mechanics* 33(1): 2-14.
22. Naffa M, Al-Gahtani HJ (2007) RBF-based meshless method for large deflection of thin plates. *Engineering Analysis with Boundary Elements*31(4): 311-317.
23. Al-Gahtani HJ, Naffa'a M (2009) RBF meshless method for large deflection of thin plates with immovable edges. *Engineering Analysis with Boundary Elements* 33(2): 176-183.
24. Xiang S, Shi H, Wang KM, Ai YT, Sha YD (2010) Thin plate spline radial basis functions for vibration analysis of clamped laminated composite plates. *European Journal of Mechanics-A/Solids*29 (5): 844-850.
25. Roque CMC, Ferreira AJM, Neves AMA, Soares CMM, Reddy JN, et al. (2011) Transient analysis of composite plates by radial basis functions in a pseudospectral framework. *Computers & Structures*89(1-2): 161-169.
26. Roque CMC, Cunha D, Shu C, Ferreira AJM (2011) A local radial basis functions-finite differences technique for the analysis of composite plates. *Engineering Analysis with Boundary Elements*35(3): 363-374.
27. Ferreira AJM, Roque CMC, Neves AMA, Jorge RMN, Soares CMM, et al. (2011) Buckling analysis of isotropic and laminated plates by radial basis functions according to a higher-order shear deformation theory. *Thin-Walled Structures* 49(7): 804-811.
28. Hussein Al-Tholaia MM, Jubran Al-Gahtani H (2015) RBF based meshless method for large deflection of elastic thin plates on nonlinear foundations. *Engineering Analysis with Boundary Elements* 51: 146-155.
29. Mohammed M, Hussein Al-Tholaia H, Jubran Al-Gahtani H (2015) RBF-Based Meshless Method for Large Deflection of Elastic Thin Rectangular Plates with Boundary Conditions Involving Free Edges. Hindawi Publishing Corporation. *Mathematical Problems in Engineering*10(51): 146-155.
30. Franke R (1982) Scattered data interpolation: tests of some methods. *Math Comp* 48: 181-200.
31. Kansa EJ, Carlson RE (1992) Improved accuracy of multiquadric interpolation using variable shape parameters. *Comput Math Applic* 24: 99-120.
32. Rippa S (1999) An algorithm for selecting a good value for the parameter c in radial basis function interpolation. *Adv Comput Math* 11 (1999): 193-210.
33. Sarra S, Sturgill D (2009) A random variable shape parameter strategy for radial basis function approximation methods. *Engineering Analysis with Boundary Elements* 33(11): 1239-1245.
34. Nojavan H, Abbasbandy S, Allahviranloo T (2017) Variable Shape Parameter Strategy in Local Radial Basis Functions Collocation Method for Solving the 2D Nonlinear Coupled Burgers Equations. *Mathematics* 5(3): 38.



This work is licensed under Creative Commons Attribution 4.0 License
DOI: [10.19080/CERJ.2019.07.555724](https://doi.org/10.19080/CERJ.2019.07.555724)

**Your next submission with Juniper Publishers
will reach you the below assets**

- Quality Editorial service
 - Swift Peer Review
 - Reprints availability
 - E-prints Service
 - Manuscript Podcast for convenient understanding
 - Global attainment for your research
 - Manuscript accessibility in different formats
- (Pdf, E-pub, Full Text, Audio)**
- Unceasing customer service

Track the below URL for one-step submission

<https://juniperpublishers.com/online-submission.php>